Applied Energy 150 (2015) 128–137

Contents lists available at ScienceDirect

Applied Energy

journal homepage: www.elsevier.com/locate/apenergy

Production of jet and diesel biofuels from renewable lignocellulosic biomass

Yajing Zhang [a], Peiyan Bi [a], Jicong Wang [a], Peiwen Jiang [a], Xiaoping Wu [a], He Xue [a], Junxu Liu [a], Xiaoguo Zhou [b,*], Quanxin Li [a,*]

[a] Department of Chemical Physics, Anhui Key Laboratory of Biomass Clean Energy, University of Science & Technology of China, Hefei 230026, PR China
[b] Hefei National Laboratory for Physical Sciences at the Microscale, Department of Chemical Physics, University of Science and Technology of China, Hefei, Anhui 230026, PR China

HIGHLIGHTS

- A novel controllable transformation of biomass into bio-jet fuels was demonstrated.
- Production of C8–C15 hydrocarbons was achieved by alkylation using ion liquid.
- Sawdust-derived biofuels basically met main technical requirements of jet fuels.

GRAPHICAL ABSTRACT

A new controlled conversion of lignocellulose biomass to bio-jet and diesel fuels by catalytic pyrolysis of biomass into low carbon hydrocarbons coupled with alkylation of aromatics.

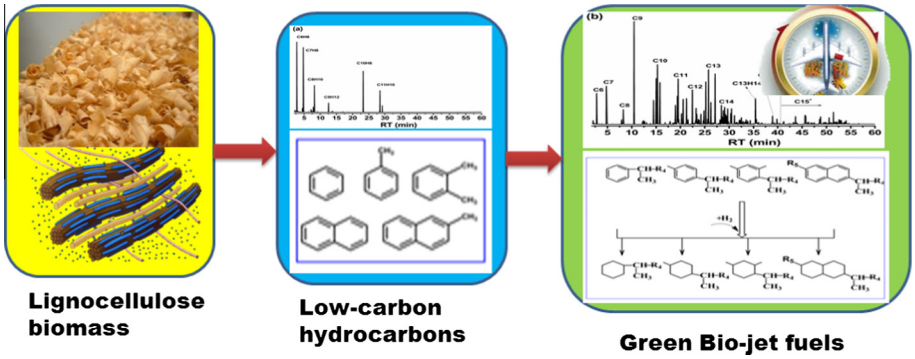

ARTICLE INFO

Article history:
Received 27 January 2015
Received in revised form 6 April 2015
Accepted 7 April 2015

Keywords:
Lignocellulose biomass
Bio-jet fuels
C8–C15 aromatics
C8–C15 cyclic alkanes
Alkylation

ABSTRACT

The continual growth in commercial aviation fuels and more strict environmental legislations have led to immense interest in developing green aviation fuels from renewable lignocellulosic biomass. This work demonstrated a novel transformation of biomass into bio-jet and diesel fuels. The transformation included following three reaction steps: (i) the catalytic pyrolysis of sawdust into low-carbon aromatics, (ii) the production of C8–C15 aromatics by the aromatic alkylation and (iii) the production of C8–C15 cyclic alkanes by the hydrogenation of C8–C15 aromatics. The production of the desired C8–C15 aromatics with the highest selectivity of 92.4% was achieved by the low temperature alkylation reactions of the low carbon aromatics using the ionic liquid of [bmim]Cl–2$AlCl_3$ (1-butyl-3-methylimidazolium chloroaluminate). The biofuels derived from sawdust basically met the main specifications of jet fuels. This transformation potentially provides a useful avenue for the development of green aviation biofuels utilizing lignocellulose biomass.

1. Introduction

Jet fuel or aviation turbine fuel is a type of aviation fuel designed for use in aircraft powered by the gas-turbine engines.

* Corresponding authors. Tel.: +86 551 63601118; fax: +86 551 63606689.
E-mail addresses: xzhou@ustc.edu.cn (X. Zhou), liqx@ustc.edu.cn (Q. Li).

http://dx.doi.org/10.1016/j.apenergy.2015.04.023
0306-2619/

The most commonly used fuels for commercial aviation are produced from petroleum refining with the standardized international specifications [1]. Over the past decade, the development of new generation hydrocarbon biofuels from renewable biomass has stimulated significant interest because of the continual growth in commercial traffic fuels and their potential environmental benefits [1–8].

To meet the challenges associated with producing bio-jet fuels from biomass, new or improved technologies are needed. Two representative technologies, catalytic hydrotreating of vegetable oils [3,5,6,9–14] and Fischer Tropsch synthesis using biomass-derived syngas [1,4,15–20], have been developed for producing green aviation bio-fuels. Catalytic hydrotreating of vegetable oils and related feedstocks can transform the triglycerides-based oils into liquid alkanes in the diesel and/or jet fuel ranges. Generally, triglycerides extracted from plant or animal oils are hydrotreated over noble metal supported or metal sulfide supported catalysts under high hydrogen pressures. Such transformation typically involves the formation of free fatty acids (FFA) by breaking the C–O bonds of the triglycerides, followed by the deoxygenation of FFA to form linear n-alkanes and the formation of lighter iso-alkanes by isomerization or cracking. The low-temperature hydrotreating (typically at 300–350 °C) mainly produce C15–C18 alkanes in the diesel range, and the cracking and isomerization at higher temperatures are generally required to improve the yield of iso-alkanes in the kerosene range [3,5,12]. So far, the synthetic paraffinic kerosenes (SPKs) produced from triglyceride-based vegetable oils have been approved for use in commercial aircraft in a 50/50 blend with petroleum-derived jet fuels [5].

Alternatively, Fischer–Tropsch synthesis (FTS) is a highly developed route to convert lignocellulose biomass into liquid alkanes used as transportation fuels [1,4,15–20]. The production of biofuels by FTS generally includes the preparation of synthesis gas by biomass gasification, cleaning and conditioning of crude bio-syngas, Fischer–Tropsch synthesis and subsequent upgrading of fuels [1,4]. The liquid products derived from FTS primarily consist of the five families of hydrocarbon groups (paraffins, iso-paraffins, olefins, aromatics and naphthenes) alone with oxygenates [1,4,15–20]. To produce acceptable jet range fuels, the raw FTS fuels must be further upgraded by subsequent hydrocracking, isomerizing and distillating [1,4,15]. Since most of the liquid hydrocarbons produced by FTS are paraffins and olefins, naphthenes and aromatics should be increased in the FTS-derived fractions to meet the specific requirement of jet fuels [16–20]. Currently, FTS-derived SPKs have been also approved for a 50/50 blend of SPKs with petroleum derived jet fuels [1,18–19].

Chemically, main compositions of commercial and military jet fuels can be described as paraffins, cyclic alkanes and aromatics, typically ranging from C8 to C15 hydrocarbons [4,15,19,21]. As mentioned above, triglycerides or FTS derived SPKs are currently utilized as the component of alkanes in commercial jet-fuels. Recently, the aromatization of propane obtained from triglycerides hydrogenolysis has been proposed to supply aromatics for blending issues in renewable jet fuels production from vegetable and algal oil [22,23]. However, directional transformation of lignocellulose biomass into C8–C15 cyclic alkanes and aromatics is still a challenging task. For example, the liquid products produced by pyrolysis of lignocellulosic biomass are generally dominated by oxygenated organics (named as bio-oils), which are not suitable for engine applications due to high viscosity, high acidity, low stability and heating value in bio-oils [24–27]. Even though the catalytic pyrolysis of lignocellulose biomass over zeolites is regarded as a cheaper route for converting biomass to hydrocarbons, main products formed from this process are typically low carbon hydrocarbons which do not meet the specific requirement of jet fuels [28,29].

The purpose of this work is to transform sawdust into jet and diesel fuels range hydrocarbons. This transform includes the production of C8–C15 aromatics by the catalytic pyrolysis of biomass coupled with the alkylation of aromatics, and the production of C8–C15 cycloparaffins by the hydrogenation of aromatics. Owing to the unique properties of ionic liquids (ILs) like low vapor pressure, high stability, nonflammability and having Bronsted and Lewis acid, ILs have attracted wide interest in organic synthesis, catalysis, separation, extraction, electrochemistry and polymerization reactions [30–34]. Present work also demonstrated that the production of the desired C8–C15 aromatics from sawdust can be achieved by the low temperature alkylation of aromatics using the [bmim]Cl–2$AlCl_3$ ionic liquid.

2. Materials and methods

2.1. Materials

The biomass material (sawdust), purchased from Anhui Yineng Bio-energy Co. Ltd. (Hefei, China), was sieved to obtain particle sizes <0.3 mm. The elemental compositions in the dried and ash free biomass mainly consists of 46.20 wt% carbon, 6.02 wt% hydrogen, 47.30 wt% oxygen and 0.48 wt% nitrogen, measured by an elemental analyzer (Vario EL-III, Elementar, Germany). All analytical reagents used were purchased from Sinopharm Chemical Reagent Company (Shanghai, China).

2.2. Catalyst preparation and characterization

The HZSM-5 zeolite with Si/Al ratio of 25 was prepared by the conversion of the sodium form (supplied by Nankai University catalyst Co., Ltd., Tianjin, China) to the protonated form via NH_4^+ exchange procedure, followed by calcination in air at 550 °C for 4 h. For the preparation of the [bmim]Cl–2$AlCl_3$ (1-butyl-3-methylimidazolium chloroaluminate) ionic liquid, 1-butyl-3-methylimidazolium chloride ([bmim]Cl) was first prepared by the following procedures. The dried and redistilled N-methylimidazolium and 1-chlorobutane were placed into a dry round-bottomed flask equipped with a reflux cooler and a magnetic agitator. The mixture was heated and reacted under the temperature of 80–85 °C for 24 h. Then the mixture was cooled to room temperature, and the unreacted reactants were removed using a rotary evaporator. The resulting imidazolium salt was washed using acetonitrile as solvent, and dried in a vacuum drying box to remove the residual solvent and water. Finally, the [bmim]Cl–2$AlCl_3$ ionic liquid was prepared by slowly adding the dried aluminum chloride to the imidazolium salt with a molar ratio of 2.0 between $AlCl_3$ and [bmim]Cl and stirring overnight at room temperature. The Pd/AC catalyst used for the hydrogenation of aromatics was prepared by the incipient wetness impregnation of the HNO_3-treated AC (active carbon) with the H_2PdCl_4 solution ($PdCl_2$ dissolved in HCl solution). The impregnated product was dried at 120 °C for 24 h, and finally reduced by H_2 (60 mL/min) at 280 °C for 8 h.

Acidity characterizations of the ionic liquid were conducted by infrared spectroscopy (Bruker Tensor 27 FT-IR spectrometer) using pyridine as a probe molecule of Lewis and Bronsted acid at room temperature. The samples were prepared by mixing pyridine and the ionic liquids in the volume ratio of 5:1, and then smeared into the liquid films on the KBr windows. The FT-IR spectrum was acquired at 1 cm^{-1} resolution using 16 scans for each sample. The NMR measurements were carried out on a high-resolution liquid nuclear magnetic resonance spectrometer (Bruker Avance 300 MHz). The HZSM-5 catalyst was characterized by NH_3-TPD (temperature programmed desorption of ammonia), XRD (X-ray

diffraction), and N_2 adsorption/desorption isotherms analysis, as the same procedures described in our previous papers [29,35–38]. The metal contents in the Pd/AC catalyst were measured by inductively coupled plasma and atomic emission spectroscopy (ICP/AES, Atomscan Advantage, Thermo Jarrell Ash Corporation, USA). The temperature programmed oxidation (TPO) analyses for determining the carbon deposited on the used catalysts were conducted in a Q5000IR thermogravimetric analyzer (USA). The samples were heated from room temperature to 900 °C with a heating rate of 10 °C/min under the air.

2.3. Experimental procedures

2.3.1. Catalytic pyrolysis of biomass

For the first step, the production of low-carbon aromatic hydrocarbons by the catalytic pyrolysis of sawdust was performed in the catalytic pyrolysis reactor, using the procedures described in our previous paper [39]. Briefly, the system was mainly composed of a tube reactor, a feeder for solid reactants, two condensers and a gas analyzer. Before each run, the reactor was flushed with nitrogen at a flow rate of 300 cm^3/min for 2 h, and was externally heated to the given temperature by the carborundum heater. Sawdust was mixed with the HZSM-5(25) catalyst with a typical catalyst/sawdust weight ratio of 2. Then the solid mixture (sawdust and catalyst) was fed into the reactor by the feeder. The liquid products in each test were collected by a condenser immersed in the ice/salt bath, and then weighed. The solid samples collected were sieved and separated into the catalyst and char/coke, and the gas in each test was collected with air bags and analyzed using a gas chromatograph (see Section 2.3.4).

2.3.2. Alkylation of biomass-derived aromatics

For producing C8–C15 aromatic hydrocarbons, in the second step, the alkylation of the low carbon aromatics produced in the first step (catalytic pyrolysis of sawdust) was carried out using the ionic liquid catalyst of [bmim]Cl–2$AlCl_3$ under the low temperature. To maximize the use of biomass feedstock, the mixture gas of C2–C4 light olefins (containing 10.46 vol.% C_2H_4, 17.17 vol.% C_3H_6 and 4.0 vol.% C_4H_8) was used as the alkylating agent, which were simulated the gas components produced by the catalytic cracking of bio-oil at 550 °C [29]. The alkylation reactions were run in batch mode in a 50 mL three-necked flask reactor equipped with a gas-inlet, a reflux cooler, sampling exit and a magnetic stirrer. The reaction temperature was controlled in the range of 25–80 °C by a thermostatic water bath with a temperature controller. For a typical run, the ionic liquid and the sawdust-derived monomers with the ionic liquid/oil ratio of 0.2 was added into the reactor, and flushed with nitrogen at a flow rate of 300 cm^3/min under the room temperature for 60 min. On reaching to the given temperature, the light olefins mixed gases with a flow rate of 30 cm^3/min was fed into the reactor, which was controlled by a mass-flow controller. Then, the reaction mixtures were stirred at 500 rpm and reacted at 25–80 °C for a given time (20–240 min). Finally, the alkylated products on the upper layer were separated from the ionic liquid catalyst at the bottom of the flask by decantation, and measured by GC–MS and other analysis (see Section 2.3.4).

2.3.3. Hydrogenation of aromatics

To produce the C8–C15 cyclic alkanes, the hydrogenation of the alkylated products (formed in the second step) was further performed in a 100 mL Parr reactor in the range of 120–200 °C for 6 h (named as the third step). For each run, the 5 wt% Pd/AC catalyst and the alkylated products with a ratio of 1:10 were used for the hydrogenation treatment. During the reaction, H_2 was added from time to time to keep the total pressure at 5 MPa. After the hydrogenation treatment, the catalyst was removed by filtration, and the resulting liquid products were weighted and further analyzed as described below.

2.3.4. Analytical methods

The liquid products collected in each test were weighed to obtain the mass of liquid products. Total carbon content in the liquid products was measured by a Vario EL III elemental analyzer. The water content was analyzed by a moisture analyzer (Model ZSD-1, Shanghai, China). The main components of the organic liquid products were analyzed by GC–MS (Thermo Trace GC/ISQ MS, USA; FID detector with a TR-5 capillary column). The moles of main organic liquid products were determined by the normalization method with standard samples. The gas in each test was collected with air bags, and analyzed using a gas chromatograph (GC-SP6890, Shandong Lunan Ruihong Chemical Instrument Co., Ltd., Tengzhou, China) with two detectors: a TCD (thermal conductivity detector) for analysis of H_2, CO, CH_4 and CO_2 separated on TDX-01 column, and a FID (flame ionization detector) for gas hydrocarbons separated on Porapak Q column. The moles of all gas products were determined by the normalization method with standard gas. The solid residues produced during the catalytic pyrolysis of sawdust were weighed, and then measured by the TGA analysis (Q5000IR thermogravimetric analyzer, USA). The yield, conversion, selectivity and distribution of products in each test were calculated as described in our previous papers [28,39]. Moreover, the specific fuel properties of the synthesized biofuels were evaluated based on the method described in the literatures [3,19]. All the tests were repeated three times and the reported data are the mean values of three trials. The standard deviations (or relative standard deviations) and the analyses of mass balance (or carbon balance) were evaluated for each test.

3. Results and discussion

3.1. Catalytic pyrolysis of biomass into low carbon aromatic hydrocarbons

To produce jet fuel range hydrocarbons from lignocellulose biomass, the catalytic depolymerization and deoxygenation of biomass are needed. Table 1 shows the influence of temperature on the production of low-carbon aromatics by the catalytic pyrolysis of sawdust over the selected HZSM-5(25) catalyst. Increasing temperatures (below 500 °C) enhanced the catalytic pyrolysis of sawdust and improved the overall yield of aromatics. At temperatures over 500 °C, the yield of aromatic hydrocarbons was reduced due to the secondary cracking of hydrocarbons. This implies that higher temperatures not only enhance depolymerization and deoxygenation of biomass, but also increase the secondary cracking of organics to form smaller molecular compounds like gas alkanes and olefins. Taking into account that the pyrolysis of biomass mainly produced oxygenated organic compounds, the presence of the zeolite catalyst promoted the deoxygenation of oxygenates into hydrocarbons. An efficient deoxygenation was nearly accomplished over HZSM-5(25) up to 500 °C, where oxygen in sawdust was removed by the formation of CO, CO_2 and H_2O.

As shown in Table 1, main organic products derived from the catalytic pyrolysis of sawdust consist primarily of the monocyclic low-carbon aromatics having 6–8 carbon atoms (like benzene, toluene and xylenes), formed from depolymerization of biomass alone with further deoxygenation and aromatization over the acidic sites of the zeolite catalyst. The selectivity of overall C6–C8 aromatics increased from 66.8 C mol% to 79.4 C mol% with increasing temperature from 450 °C to 600 °C. It was noticed that lighter aromatics like benzene increased with increasing temperature in parallel with the decrease in the heavier aromatics like xylenes

Table 1
Catalytic pyrolysis of sawdust into the low-carbon aromatics over HZSM-5(25) under the reaction conditions: 450–600 °C, N_2 flow speed of 300 cm^3 min^{-1}, and the catalyst/sawdust mass ratio of 2.

Temperature	450 °C	500 °C	550 °C	600 °C
Aromatics carbon yield (C mol%) [a]				
C6–C8 aromatics	18.7	21.4	18.3	17.2
C9 aromatics	2.2	1.3	0.9	0.8
Naphthalenes/indenes	5.1	5.9	4.8	3.5
Oxygenates	1.8	0.3	0.2	–
Others	1.2	0.9	0.7	0.3
Aromatics selectivity (C mol%) [b]				
C6–C8 aromatics	66.8	71.1	74.3	79.4
C9 aromatics	5.7	3.8	3.0	2.8
Naphthalenes/indenes	17.2	19.8	18.6	16.0
Oxygenates	6.3	2.2	1.1	–
Others	4.0	3.0	2.7	1.5
Liquid products distribution (wt%) [c]				
Benzene	11.5	21.7	28.7	39.8
Toluene	19.7	30.9	32.0	28.7
Xylenes	33.3	18.4	13.9	12.0
C9 aromatics	6.1	3.9	3.3	2.8
Naphthalenes/indenes	17.0	19.0	18.1	15.8
Oxygenates	7.5	2.6	1.6	–
Others	4.8	3.3	2.4	0.8
Overall weight yields (wt%) [d]				
Organic liquid	14.5	14.7	12.2	10.9
Water	24.3	25.7	26.1	28.3
Gas	23.1	28.3	37.4	45.6
Solid residues	27.5	22.5	17.9	16.6
Sum	89.4	91.2	93.6	101.4

[a] The values are averages of three trials with relative standard deviations <13.1%.
[b] The values are averages of three trials with relative standard deviations <12.5%.
[c] The values are averages of three trials with relative standard deviations <11.4%.
[d] The values are averages of three trials with relative standard deviations <12.8%.
The mass balance ranged from 89.4% to 101.4%.

due to the removal of the alkyl groups in the heavier aromatics at higher temperatures. Smaller amounts of polycyclic aromatic hydrocarbons such as naphthalene and methylnaphthalene were likely produced by the oligomerization reactions of lighter aromatics. The gas products mainly consist of CO, CO_2 and CH_4 together with smaller amount of C_2–C_4 alkanes and $C_2^=$–$C_4^=$ olefins. The positive temperature dependence of the gas yield reflects that the biomass gasification, deoxygenation as well as the cracking of oxygenats are increased at higher temperatures. To maximize the production of the liquid bio-fuels, the sawdust-derived oil obtained at 500 °C was used in the subsequent alkylation step.

3.2. Production of C8–C15 aromatic hydrocarbons by low-temperature alkylation

To produce hydrocarbons in the jet fuel range, the transformation of sawdust-derived low carbon hydrocarbons into C8–C15 aromatic hydrocarbons was conducted by means of the low temperature alkylation of aromatics using the [bmim]Cl–$2AlCl_3$ ionic liquid. Table 2 presents the effect of temperature on the conversion of low carbon aromatics, the selectivity and the distributions of hydrocarbons in the resulting biofuels. The [bmim]Cl–$2AlCl_3$ ionic liquid shows high catalytic activity and selectivity of C8–C15 aromatics for the low temperature alkylation of low carbon aromatics. Even at the room temperature (25 °C), the conversions of the monocyclic aromatic hydrocarbons (MAHs) and polycyclic aromatic hydrocarbon (PAHs) reached about 68.5% and 78.6% respectively, alone with a high C8–C15 aromatics selectivity of 92.4%. For different low carbon aromatics, the alkylation reactions of aromatics are somewhat associated with the alkyl groups on the aromatic ring. For example, the conversion of benzene is slightly higher than that of toluene, which is most likely caused by the steric effect of the substituent alkyl groups on the aromatic

Table 2
Effect of temperature on producing C8–C15 hydrocarbons by the alkylation of the low-carbon aromatics using [bmim]Cl–$2AlCl_3$ at 25–80 °C for 60 min.

Temperature (°C)	25	40	50	60	70	80
Conversion (C mol%)[a]						
C6–C8 aromatics	68.5	75.4	82.5	85.3	78.2	77.7
Naphthalenes/indenes	78.6	87.3	89.1	94.0	96.3	97.2
C2–C4 olefins	73.2	77.4	78.2	80.6	76.9	75.4
Selectivity (C mol%)[b]						
C8 aromatics	2.5	2.3	2.0	1.8	2.0	2.1
C9 aromatics	11.1	10.3	9.3	8.1	7.2	7.0
C10 aromatics	21.3	18.3	17.2	15.0	14.5	14.1
C11 aromatics	12.8	13.1	12.2	13.1	12.8	13.3
C12 aromatics	10.9	9.9	8.9	9.3	9.1	8.9
C13 aromatics	14.9	14.3	14.2	13.8	13.6	12.6
C14 aromatics	15.9	14.9	16.0	16.8	15.0	12.0
C15 aromatics	3.0	4.5	5.3	5.7	6.3	6.9
$C15^+$ aromatics	7.6	12.4	14.9	16.4	19.5	23.1
Distribution of MAHs (wt%) [c]						
C6 aromatics	4.9	4.0	3.4	2.7	4.0	3.8
C7 aromatics	5.6	4.2	3.6	3.0	4.9	5.1
C8 aromatics	5.0	4.7	4.4	4.0	4.3	4.6
C9 aromatics	9.2	8.8	8.3	7.4	6.3	6.1
C10 aromatics	15.5	14.8	14.7	13.3	12.5	12.2
C11 aromatics	10.0	10.9	10.7	11.8	11.2	11.6
C12 aromatics	8.7	8.4	8.0	8.5	8.1	7.9
C13 aromatics	8.1	9.3	9.7	10.0	9.5	10.2
C14 aromatics	9.3	10.8	11.3	12.2	9.5	8.5
C15 aromatics	2.3	3.5	4.2	4.8	5.0	5.3
$C15^+$ aromatics	3.9	4.6	5.4	5.9	6.8	7.7
Distribution of PAHs (wt%) [c]						
C10 PAHs	1.4	0.9	0.8	0.4	0.3	0.2
C11 PAHs	0.5	0.4	0.3	0.2	0.1	0.1
C12 PAHs	0.3	0.2	0.1	0.1	–	–
C13 PAHs	5.0	4.0	3.1	2.7	2.5	1.0
C14 PAHs	4.7	3.1	3.2	3.3	3.8	2.1
C15 PAHs	0.2	0.4	0.6	0.5	0.6	0.8
$C15^+$ PAHs	5.4	7.0	8.2	9.2	10.6	12.8

[a] The values are averages of three trials with relative standard deviations < 8.8%.
[b] The values are averages of three trials with relative standard deviations < 10.9%.
[c] MAHs: monocyclic aromatic hydrocarbons. PAHs: polycyclic aromatic hydrocarbons. The values are averages of three trials with relative standard deviations < 10.2%. The mass balance ranged from 90.2% to 99.9%.

ring. The conversion of PAHs like naphthalene and methylnaphthalene, on the other hand, is obviously higher than the conversion of MAHs. This observation could be attributed to that PAHs have higher electron density, and thereby, show higher electrophilic substitution reactivity as compared with MAHs. As the temperature increased from 25 °C to 60 °C, the conversion of C6–C8 aromatics was improved from 68.5% to 85.3%. The selectivity of overall C8–C15 aromatics, on the other hand, decreased from 92.4% to 76.9% with increasing temperatures from 25 °C to 80 °C. Since the aromatic alkylation is an exothermic reaction, increasing temperature results in the decrease of equilibrium constants and is not beneficial to the aromatic alkylation. On the other hand, higher temperatures are conducive to overcome the activation energy required to the alkylation reactions of aromatics. Meanwhile, the collision probability between ionic liquid and reactants will be enhanced at higher temperatures, leading to the increase in the reaction rates of the aromatic alkylation. Moreover, the contents of the main alkylation products (C8–C15 aromatic hydrocarbons) were decreased from 80.2 wt% to 70.6 wt% as increasing temperatures from 25 °C to 80 °C. Since the alkylation of aromatics is a consecutive reaction process, the primary alkylation products can be multiply alkylated to form high carbon number aromatics, leading to the rise in the heavier aromatic hydrocarbons at higher temperatures.

Table 3 shows the influence of the reaction time on the alkylation of the sawdust-derived low carbon aromatics. Increasing reaction time improved the overall alkylation efficiency of the low-carbon aromatics. After the alkylation reactions at

Table 3
Effect of reaction time on producing C8–C15 hydrocarbons by the alkylation of sawdust-derived monomers using [bmim]Cl–2AlCl$_3$ at 60 °C for 20–240 min.

Time (min)	20	40	60	90	120	240
Conversion (C mol%)[a]						
C6 aromatics	64.3	75.5	87.8	93.1	96.1	100
C7 aromatics	53.2	61.9	85.9	89.8	93.9	100
C8 aromatics	42.2	50.9	80.3	80.3	84.6	95.1
C6-C8 aromatics	54.9	64.6	85.3	88.9	92.6	98.9
Naphthalenes/indenes	78.4	87.9	94.0	99.9	100	100
C2–C4 olefins	85.5	81.6	80.6	75.3	71.2	64.2
Selectivity (C mol%)[b]						
C8 aromatics	5.8	4.3	1.8	2.8	2.0	0.5
C9 aromatics	12.0	10.2	8.1	7.7	5.3	1.2
C10 aromatics	19.1	17.6	15.0	11.2	5.5	1.0
C11 aromatics	18.6	15.2	13.1	10.5	6.2	0.9
C12 aromatics	12.7	9.3	9.3	9.7	9.2	1.0
C13 aromatics	11.6	14.5	13.8	13.8	12.2	4.1
C14 aromatics	12.1	16.2	16.8	16.9	22.8	2.3
C15 aromatics	3.3	3.8	5.7	6.5	11.1	12.3
C15$^+$ aromatics	4.8	8.8	16.4	20.9	25.7	76.7
Distribution of monocyclic aromatic hydrocarbons (wt%) [c]						
C6 aromatics	9.4	6.2	2.7	1.4	0.8	–
C7 aromatics	11.9	9.3	3.0	2.0	1.2	–
C8 aromatics	10.4	8.5	4.0	6.5	4.6	1.1
C9 aromatics	8.7	8.1	7.4	7.1	5.0	1.2
C10 aromatics	12.2	12.8	13.3	10.3	5.2	1.0
C11 aromatics	12.5	11.8	11.8	9.7	5.9	0.9
C12 aromatics	8.5	7.2	8.5	9.0	8.8	1.0
C13 aromatics	3.1	7.0	10.0	10.7	9.3	2.9
C14 aromatics	5.5	9.0	12.2	12.9	19.6	2.0
C15 aromatics	1.2	2.1	4.8	5.7	9.9	12.1
C15$^+$ aromatics	–	1.6	5.9	7.9	12.4	60.3
Distribution of polycyclic aromatic hydrocarbons (wt%) [c]						
C10 PAHs	1.6	1.1	0.4	–	–	–
C11 PAHs	1.0	0.3	0.2	–	–	–
C12 PAHs	0.8	0.2	0.1	–	–	–
C13 PAHs	5.2	4.5	2.7	2.1	2.3	1.1
C14 PAHs	3.3	3.9	3.3	2.8	2.2	0.3
C15 PAHs	1.2	0.9	0.5	0.4	0.7	0.1
C15$^+$ PAHs	3.5	5.5	9.2	11.5	11.5	16.0

[a] The values are averages of three trials with relative standard deviations <9.2%.
[b] The values are averages of three trials with relative standard deviations <10.6%.
[c] The values are averages of three trials with relative standard deviations <9.9%.
The mass balance ranged from 90.7% to 100.3%.

typical temperature of 60 °C for 240 min, almost all of low carbon aromatics were converted higher carbon number aromatics. With increasing reaction time, the distribution of the carbon number in the resulting biofuels significantly shifted toward the heavier aromatics, indicating that the secondary alkylations of aromatics were enhanced for longer reaction duration. Accordingly, the carbon number distribution of aromatic hydrocarbons was able to be efficiently tuned into the desired range of C8–C15 by the reaction temperature and time during the alkylation of aromatics using the ionic liquid catalyst. The adjustment of the carbon number distribution in the liquid biofuels by the reaction time (Table 3) is more sensitive as comprised with turning temperature (Table 2). For example, the resulting biofuel after the alkylation of low carbon aromatics under the optimal experimental condition (60 °C for 60 min) contains 79.2 wt% C8–C15 aromatic hydrocarbons in the jet fuel range. On the other hand, the biofuel derived from the alkylation of low carbon aromatics at 60 °C for 240 min contains 76.3 wt% C15$^+$ aromatic hydrocarbons in the diesel range.

3.3. Production of C8–C15 cyclic alkanes through hydrogenation of aromatics

Cyclic alkanes is the second most abundant components required in the commercial and military jet fuels with the mass percent of 20–50 wt% [19,40,41]. Here, the production of the C8–C15 cyclic alkanes was conducted by the hydrogenation of the C8–C15 aromatics. As shown in Table 4, the conversions of the monocyclic aromatic hydrocarbons (MAHs) and polycyclic aromatic hydrocarbons (PAHs) at the lower temperature of 120 °C were about 49.3% and 98.6% respectively, alone with a 67.7% selectivity of C8–C15 cyclic alkanes. Increasing the reaction temperatures improved the hydrogenation efficiency of aromatics. Nearly all of the sawdust-derived aromatics were converted into the saturated cyclic alkanes after the hydrogenation at 200 °C for 6 h. The conversion of polycyclic aromatic hydrocarbons was higher than that of monocyclic aromatic hydrocarbons, suggesting that the activation energy required for the hydrogenation of PAHs was less than that required for the hydrogenation of MAHs. The organic liquid derived from the hydrogenation of aromatics at 200 °C for 6 h contains 80.4 wt% C8–C15 cyclic alkanes with the average molecular formulation of $C_{11.5}H_{21.5}$. Moreover, no significant change in the carbon number distribution after the hydrogenation treatment was found, as compared with the distribution before the hydrogenation of aromatics. This implies that the cracking reactions seem to be neglectable during the low temperature hydrogenation process.

3.4. Stability and reusability of catalysts

As shown in Fig. 1, the catalyst stability during the catalytic pyrolysis of sawdust over the HZSM-5(25) catalyst was tested at

Table 4
Production of C8–C15 cyclic alkanes by the hydrogenation of the sawdust-derived C8–C15 aromatics over the 5.0 wt% Pd/AC catalyst at 5 MPa for 6 h.

Temperature (°C)	120	150	180	200
Conversion (C mol%)[a]				
MAHs	49.3	65.0	88.1	100
PAHs	98.6	98.9	99.2	100
Selectivity of cyclic alkanes (Cmol%) [b]				
C6 cyclic alkanes	5.1	3.8	3.2	2.7
C7 cyclic alkanes	6.1	4.3	3.7	3.2
C8 cyclic alkanes	8.3	6.3	4.3	4.0
C9 cyclic alkanes	13.4	11.0	8.8	7.7
C10 cyclic alkanes	22.6	19.3	15.4	13.4
C11 cyclic alkanes	8.9	13.7	14.0	12.3
C12 cyclic alkanes	3.9	7.8	9.0	8.5
C13 cyclic alkanes	5.1	13.5	14.2	14.0
C14 cyclic alkanes	4.7	4.8	14.8	15.3
C15 cyclic alkanes	0.8	0.7	2.2	5.2
C15$^+$ cyclic alkanes	9.2	10.5	10.2	13.7
Distribution of monocyclic alkanes (wt%) [c]				
C6 monocyclic alkanes	2.6	2.5	2.8	2.7
C7 monocyclic alkanes	3.1	2.8	3.2	3.2
C8 monocyclic alkanes	4.2	4.1	3.8	4.0
C9 monocyclic alkanes	6.8	7.2	7.6	7.7
C10 monocyclic alkanes	11.2	12.1	13.0	13.0
C11 monocyclic alkanes	4.2	8.6	12.1	12.1
C12 monocyclic alkanes	2.0	5.0	7.8	8.4
C13 monocyclic alkanes	0.1	6.1	9.6	11.0
C14 monocyclic alkanes	0	0.2	9.8	12.2
C15 monocyclic alkanes	0	0	1.3	4.4
C15$^+$ monocyclic alkanes	0	0	0	5.3
Distribution of polycyclic alkanes (wt%) [c]				
C10 polycyclic alkanes	0.3	0.5	0.5	0.4
C11 polycyclic alkanes	0.3	0.3	0.2	0.2
C12 polycyclic alkanes	0	0.1	0.1	0.1
C13 polycyclic alkanes	2.5	2.7	2.8	3.0
C14 polycyclic alkanes	2.4	2.9	3.2	3.1
C15 polycyclic alkanes	0.4	0.4	0.6	0.8
C15$^+$ polycyclic alkanes	4.7	6.9	9.2	8.4

[a] MAHs: monocyclic aromatic hydrocarbons. PAHs: polycyclic aromatic hydrocarbons. The values are averages of three trials with relative standard deviations <9.5%.
[b] The values are averages of three trials with relative standard deviations <8.9%.
[c] The values are averages of three trials with relative standard deviations <10.0%.
The mass balance ranged from 91.2% to 101.4%.

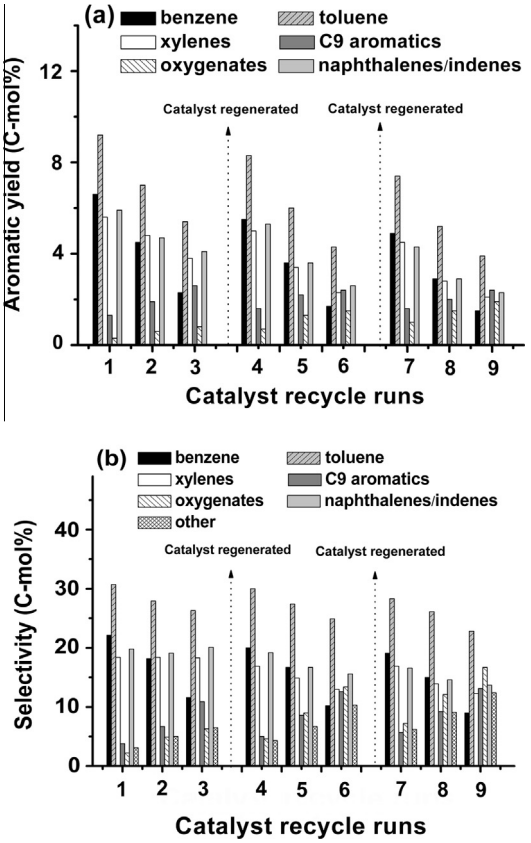

Fig. 1. Catalyst stability and reaction-regeneration cycles during the catalytic pyrolysis of sawdust over the HZSM-5 catalyst (reaction conditions: 500 °C, N_2 flow speed of 300 cm^3 min^{-1}, catalyst:sawdust = 2; regeneration conditions: 550 °C, O_2 flow speed of 300 cm^3 min^{-1}, t = 5 h). The values reported are averages of three trials and relative standard deviations were <13.6%. The mass balance ranged from 88.6% to 101.8%.

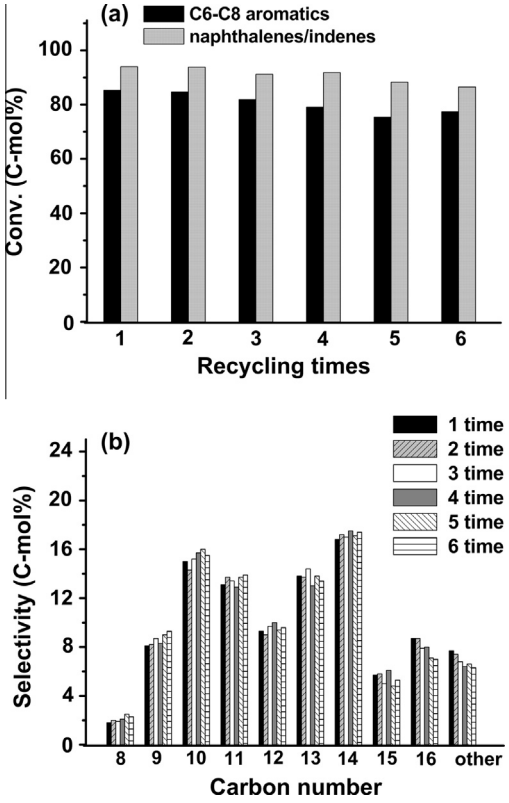

Fig. 2. Catalyst stability during the alkylation of the low-carbon aromatics using the [bmim]Cl–2$AlCl_3$ ionic liquid (reaction conditions: 60 °C for 60 min in each run. The values are averages of three trials with relative standard deviations <10.2%. The mass balance ranged from 90.2% to 100.5%.

the typical temperature of 500 °C. The regeneration cycles of catalyst were also conducted by the method of coke burn-off. After the catalyst was continuously used for three rounds without regeneration treatment, the overall yield of aromatic hydrocarbons obviously decreased. When the regenerated catalysts was reused, the selectivity of C6–C8 aromatics were also decreased, accompanied by an increase in the content of oxygenates. To further illustrate the deactivation of the catalyst, the main characteristics of the fresh, used and regenerated zeolite catalysts were investigated (Table 5). The formation of the coke on the used catalyst was also characterized by temperature programmed oxidation (Table 5). The activity decay observed during the catalytic pyrolysis of sawdust could be attributed to coke deactivation together with irreversible deactivation like the dealuminization of the zeolite and the reduction of the catalyst acidity, as proved in this work (Table 5) and in the literatures ([42,43]). The catalyst deactivation caused by the carbon deposition on the catalyst seems to be a main factor, since the activity of the used catalysts was almost recovered by treating it with oxygen at 550 °C (Fig. 1). Definitely, further study for the reduction of the coke deposition and the deactivation mechanism of the catalyst is needed in our future work.

As shown in Fig. 2, no significant changes in the catalytic activity of the [bmim]Cl–2$AlCl_3$ ionic liquid was found after the alkylation reactions of the sawdust derived low-carbon aromatics for six rounds. In addition, the Pd/AC catalyst also showed good stability during the hydrogenation of C8–C15 aromatics for an 18 h test (not shown here). The good stability of the ionic liquid catalyst and the Pd/AC catalyst should be mainly benefit from the mild operation conditions along with a negligible coke-deposition in the alkylation and hydrogenation processes.

3.5. Possible reaction pathways for formation of C8–C15 aromatics and cycloparaffins

The aim of this work was to produce two main components of jet fuels (cycloparaffins and aromatics) using sawdust. As shown Fig. 3, the transformation of biomass into the jet (or diesel) fuel

Table 5
Main characteristics of the fresh, used and regenerated catalysts of HZSM-5(25).[a]

Catalysts	Si/Al	S_{BET} m^2/g	V_p cm^3/g	Total acid mmol $NH_3/g_{cat.}$	$[C]_{deposited}$ $g_c/(g_{catalyst} \times h)$
HZSM-5	25 ± 1	282.4 ± 11.2	0.52 ± 0.07	0.58 ± 0.06	–
Used-I[b]	28 ± 2	206.3 ± 26.3	0.39 ± 0.04	0.46 ± 0.07	2.21 ± 0.18
Regenerated-I[c]	28 ± 1	225.6 ± 22.8	0.45 ± 0.03	0.47 ± 0.04	0.46 ± 0.14

[a] Symbols meanings: Si/Al (the ratio of silicon to aluminum in the zeolites), S_{BET} (Brunauer–Emmett–Teller surface area) and V_p (pore volume). $[C]_{deposited}$: carbon content deposited in the used catalyst.
[b] Used-I stands for the catalyst used for the catalytic pyrolysis of sawdust at 500 °C and nitrogen flow rate of 300 mL min^{-1} for 6 h.
[c] Regenerated-I stands for the regenerated catalyst which Used-I was regenerated at 550 °C and oxygen flow rate of 300 mL min^{-1} for 5 h.

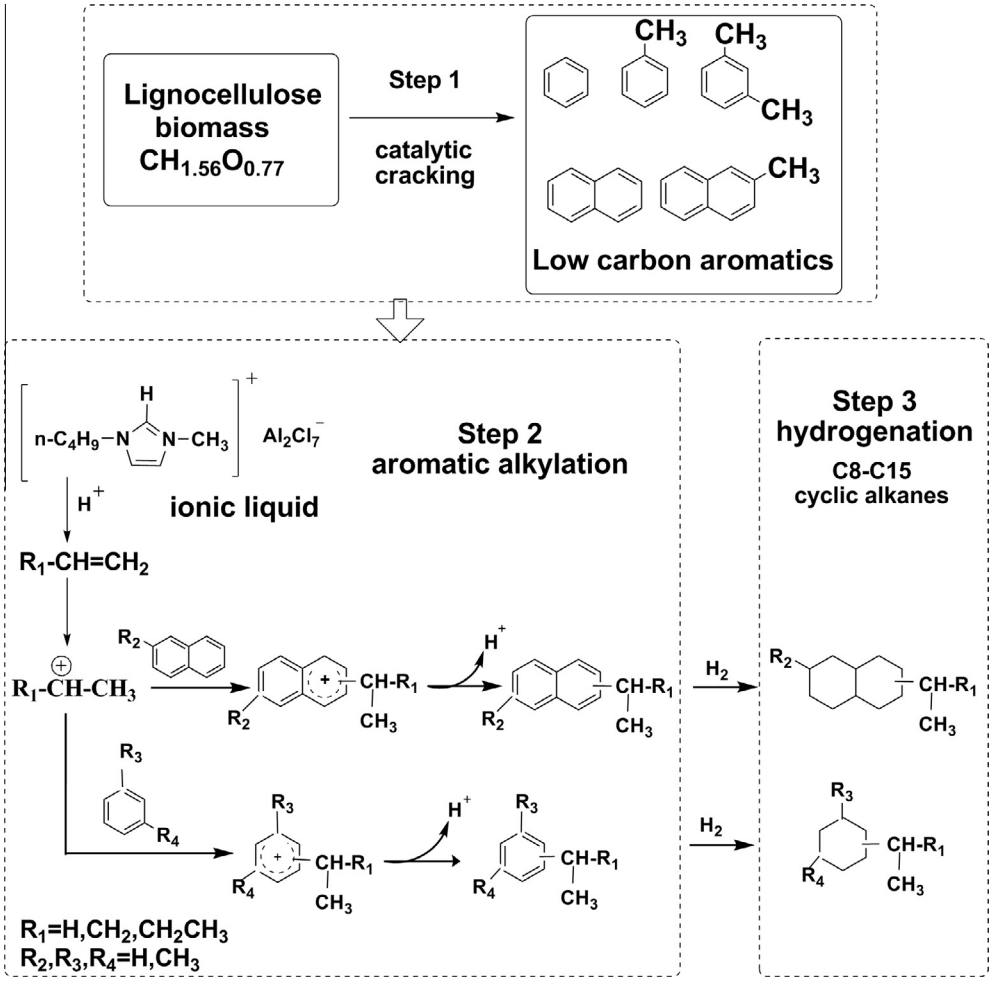

Fig. 3. Reaction pathways for the transformation of biomass into the jet (or diesel) fuel range hydrocarbons: the catalytic pyrolysis of biomass into low-carbon aromatic monomers (Step 1), the production of C8–C15 aromatics by the alkylation of aromatics using the ionic liquid (Step 2), and the production of C8–C15 cyclic alkanes by the hydrogenation of C8–C15 aromatics (Step 3).

range hydrocarbons with three reaction steps was demonstrated. In the first step, the catalytic pyrolysis of biomass to form the low-carbon aromatics was conducted using the HZSM-5 catalyst. The catalytic pyrolysis mainly involved the formation of oxygenated organic compounds by biomass depolymerization, followed by the formation of low-carbon aromatics (mainly C6–C8 monocyclic aromatic hydrocarbons) by further deoxygenation, catalytic cracking and aromatization over the acidic sites of the zeolite [28,39]. Smaller amounts of polycyclic aromatic hydrocarbons like naphthalenes were formed by the oligomerization of aromatics during the catalytic pyrolysis of biomass.

The second step involves the selective production of C8–C15 aromatic hydrocarbons by a series of alkylation reactions of low carbon aromatics with C2–C4 light olefins using the ionic liquid. The [bmim]Cl–2$AlCl_3$ ionic liquid was proved to be a high active catalyst for producing the aromatic hydrocarbons in the jet or

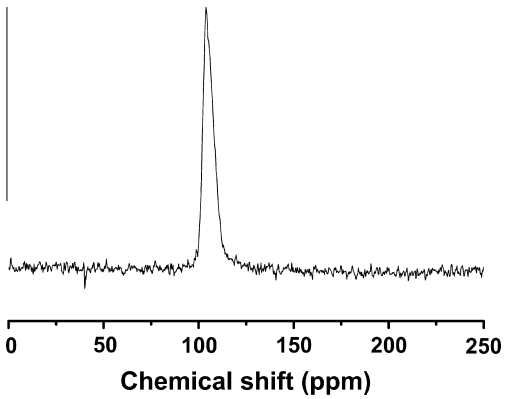

Fig. 4. Typical ^{27}Al NMR spectra of the [bmim]Cl–2$AlCl_3$ ionic liquid catalyst. The strong signal around 103 ppm belonged to $Al_2Cl_7^-$.

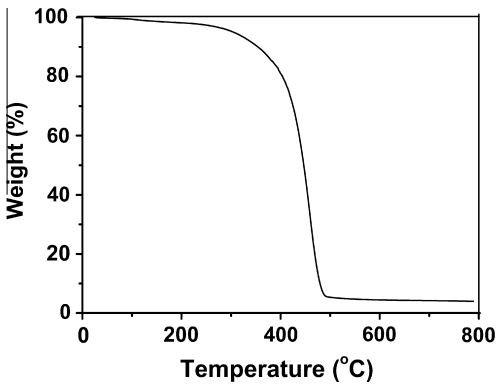

Fig. 5. Typical TGA curve of the [bmim]Cl–2$AlCl_3$ ionic liquid catalyst.

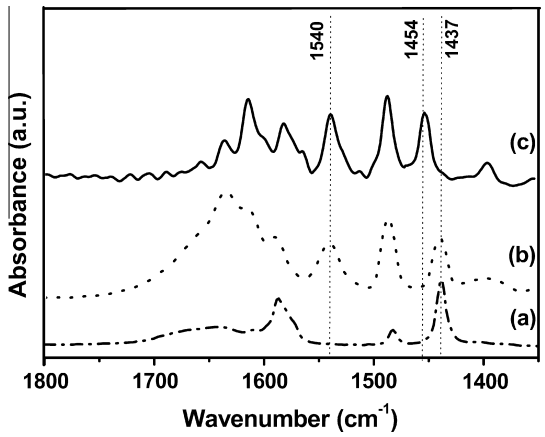

Fig. 6. FT-IR spectra of (a) pure pyridine, (b) pyridine/HCl solution and (c) pyridine/[bmim]Cl–$2AlCl_3$ ionic liquid. The bands at 1437 cm^{-1} and 1579 cm^{-1} correspond to free pyridine whilst bands of pure pyridine. The bands at 1454 cm^{-1} and 1540 cm^{-1} correspond to pyridine bonded at a Lewis acid site and pyridine bonded at a Brønsted acid site, respectively.

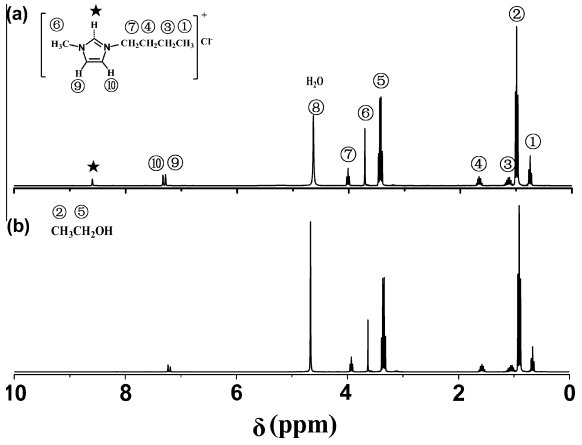

Fig. 7. H^1 NMR spectra of (a) [bmim]Cl/ethanol solution and (b) [bmim]Cl/ethanol after titrated with KOH solution. δ: chemical shift. The serial numbers represent the different H atoms in 1-butyl-3-methylimidazolium chloride [BMIM]Cl (based on Ref. [45]).

diesel range by the alkylation reactions. In particular, the carbon number distribution of aromatics can be tuned by changing the reaction temperature and time.

Chemically, the [bmim]Cl–$2AlCl_3$ ionic liquid consists of the cations of 1,3-two alkyl substituted imidazolium together with the anions of $Al_2Cl_7^-$, as demonstrated by the ^{27}Al NMR spectra (Fig. 4). The TGA results indicate that the ionic liquid had high thermal and chemical stability up to 375 °C (Fig. 5). Fig. 6 shows the typical FT-IR spectra from three samples (pyridine/[bmim]Cl–$2AlCl_3$ ionic liquid, pure pyridine and pyridine/HCl solution). For pyridine/[bmim]Cl–$2AlCl_3$ ionic liquid, the bands at 1454 cm^{-1} and 1540 cm^{-1} correspond to the characteristic peaks of Lewis acid (pyridine bonded at a Lewis acid site) and Brønsted acid (pyridine bonded at a Brønsted acid site) respectively, when pyridine was used as a probe molecule [44]. Based on the comparison of ^1H NMR spectra before and after titrated with KOH solution (Fig. 7), the absence of H in the star site after titrated with KOH solution suggests that the ionic liquid can provide protons [45]. Accordingly, the FT-IR and ^1H NMR characterizations support that the ionic liquid posses the properties of both Bronsted acid and Lewis acid. The ionic liquid could enhance the olefin protonation and the formation of active electrophilic species (positive ions of olefins), leading to the enhancement of the alkylation of low carbon aromatics with light olefins. Based on the products identified, the main reaction pathways involved in the alkylation of the sawdust-derived aromatics are illustrated in Fig. 3. The typical primary alkylation reactions can be described by the following stoichiometric expressions.

$$C_6H_6 + C_nH_{2n} \rightarrow C_6H_5{-}C_nH_{2n+1} \quad (n = 2{-}4) \tag{1}$$

$$C_6H_5{-}CH_3 + C_nH_{2n} \rightarrow CH_3{-}C_6H_4{-}C_nH_{2n+1} \quad (n = 2{-}4) \tag{2}$$

$$CH_3{-}C_6H_4{-}CH_3 + C_nH_{2n} \rightarrow (CH_3)_2{-}C_6H_3{-}C_nH_{2n+1} \quad (n = 2{-}4) \tag{3}$$

$$C_{10}H_8 + C_nH_{2n} \rightarrow C_{10}H_7{-}C_nH_{2n+1} \quad (n = 2{-}4) \tag{4}$$

Finally, the subsequent hydrogenation of the alkylated aromatics in the third step resulted in the saturation of the unsaturated aromatic hydrocarbons over the Pd/AC metal catalyst, and selectively produced the C8–C15 cyclic alkanes from the biomass-derived C8–C15 aromatics. To clarify the detailed mechanism of the aromatic alkylation and controlling step, further study on the alkylation of relative model compounds with the kinetic calculations is needed in our future work.

Table 6
Comparison of fuel properties in two sawdust-derived biofuels and commercial/military jet fuels.

Specification tests	Commercial/military jet fuels			This work	
	Jet A[a]	Jet-A1[a]	JP-8[b]	Biofuel-I[c]	Biofuel-II[d]
Heat of combustion (MJ/kg)	43.3	43.3	43.0	43.1 ± 1.2	45.9 ± 1.5
Freezing point (°C)	−40	−47	−49	<−70	<−70
Kinetic viscosity @ −20 °C (mm^2/s)	5.78	4.21	4.10	6.5 ± 0.5	7.2 ± 0.3
Specific gravity @15 °C (g/cm^3)	0.803	0.797	0.799	0.878 ± 0.03	0.823 ± 0.02
Carbon content (wt%)	86.4	86.3	86.2	89.69 ± 2.7	85.72 ± 3.4
Hydrogen content (wt%)	13.5	13.4	13.7	10.26 ± 0.41	14.28 ± 0.86
Total oxygen (wt%)	0.0044	–	–	0.033 ± 0.007	u.d.
Total sulfur (wt%)	<0.3	0.04	0.064	u.d.	u.d.
Average carbon number	11.6	11.0	10.9	11.5 ± 0.4	11.5 ± 0.7
H/C (mol ratio)	1.91	1.98	1.90	1.37 ± 0.11	1.99 ± 0.10
Average molecular formula	$C_{11.6}H_{22}$	$C_{11}H_{21}$	$C_{10.9}H_{20.9}$	$C_{11.5}H_{15.7}$	$C_{11.5}H_{21.5}$

[a] Ref. [18,40,46].
[b] Ref. [19,40].
[c] Biofuel-I: aromatics biofuel, produced by the catalytic cracking of sawdust over the HZSM-5 catalyst at 500 °C along with the alkylation of the sawdust-derived monomers using the [bmim]Cl–$2AlCl_3$ ionic liquid at 60 °C for 1 h.
[d] Biofuel-II: cyclic alkanes biofuel, produced by the hydrogenation of aromatics over the Pd/AC catalyst at 200 °C for 6 h. u.d. = undetected.

3.6. Properties of sawdust-derived biofuels

Chemically, the conventional commercial or military jet fuel produced from the petroleum refining process is a mixture of three main families of alkanes, cyclic alkanes and aromatics, typically ranging from C8 to C15 hydrocarbons [4,15,19]. The ratios of three main components depend on different commercial and military jet fuels such as Jet A1, Jet A and JP-8. Among the numerous specifications, three basic technical requirements are fuel energy density (>43 MJ/kg), freeze point (<−47 °C) and viscosity (<8 mm^2/s) [3,18–19,46].

Table 6 summarized some important properties of the biofuels synthesized in this work, which are compared with the specifications of several typical commercial and military jet fuels. Two typical sawdust-derived products (aromatics biofuel and cyclic alkanes biofuel) basically met the carbon number range and the basic technical specifications of jet fuels, when compared with the values of the commercial and military jet fuels. The typical cyclic alkanes biofuel (Biofuel-I) consists of C8–C15 cyclic alkanes of 80.4 wt% with the average molecular formulation of $C_{11.5}H_{21.5}$. Biofuel-I met the basic requirements of jet fuels based on its heat of combustion of 45.9 MJ/kg, density of 0.823 g/cm^3, viscosity of 7.2 mm^2/s and freeze point of <−70 °C. Another typical aromatics biofuel (Biofuel-II) contains C8–C15 aromatics of 79.2 wt% with the average molecular formulation of $C_{11.5}H_{15.7}$. Biofuel-II possesses a combustion heat of 43.1 MJ/kg, density of 0.878 g/cm^3 and viscosity of 6.5 mm^2/s. Moreover, sulfur content and oxygen content in the resulting products were very low. The above results clearly show that the cycloparaffinic and aromatic components required in jet fuel can be directionally synthesized using rich and renewable lignocellulosic biomass (sawdust) under the mild reaction conditions.

4. Conclusions

This work demonstrated that sawdust was able to be converted into jet and diesel fuel range hydrocarbons by a controlled transformation. The C6–C8 aromatics, produced by the catalytic pyrolysis of sawdust, were further converted to C8–C15 aromatics with a selectivity of 92.4% by the low temperature alkylation using the [bmim]Cl–$2AlCl_3$ ionic liquid. After the hydrogenation of aromatics, the resulting bio-fuel contains C8–C15 cyclic alkanes of 80.4 wt% with the average molecular formulation of $C_{11.5}H_{21.5}$. Two biomass-derived products, C8–C15 cycloparaffins and aromatics, basically met the main requirements of jet fuels. The transformation potentially provides a new and useful way for development of green aviation biofuels using lignocellulose biomass.

Acknowledgements

We acknowledge the financial support from the National Key Basic Program of China (973 Program, 2013CB228105), the National Sci-Tech Support Plan (2014BAD02B03), the National Natural Science Foundation of China (51161140331), the Program for Changjiang Scholars and Innovative Research Team in University and the Fundamental Research Funds for the Central Universities (wk 2060190040).

References

[1] Liu GR, Yan BB, Chen GR. Technical review on jet fuel production. Renew Sust Energy Rev 2013;25:59–70.
[2] Valle B, Castaño P, Olazar M, Bilbao J, Gayubo AG. Deactivating species in the transformation of crude bio-oil with methanol into hydrocarbons on a HZSM-5 catalyst. J Catal 2012;285:304–14.
[3] Verma D, Kumar R, Rana BS, Sinha AK. Aviation fuel production from lipids by a single-step route using hierarchical mesoporous zeolites. Energy Environ Sci 2011;4:1667–71.
[4] Yan QG, Yu F, Liu J, Street J, Gao JS, Cai ZY, et al. Catalytic conversion wood syngas to synthetic aviation turbine fuels over a multifunctional catalyst. Bioresour Technol 2013;127:281–90.
[5] Fortier M-OP, Roberts GW, Stagg-Williams SM, Sturm BSM. Life cycle assessment of bio-jet fuel from hydrothermal liquefaction of microalgae. Appl Energy 2014;122:73–82.
[6] Wang HL, Yan SL, Salley SO, Ng KYS. Hydrocarbon fuels production from hydrocracking of soybean oil using transition metal carbides and nitrides supported on ZSM-5. Ind Eng Chem Res 2012;51:10066–73.
[7] Chiaramonti D, Prussi M, Buffi M, Tacconi D. Sustainable bio kerosene: Process routes and industrial demonstration activities in aviation biofuels. Appl Energy 2014;136:767–74.
[8] Hari TK, Yaakob Z, Binitha NN. Aviation biofuel from renewable resources: routes, opportunities and challenges. Renew Sust Energy Rev 2015;42:1234–44.
[9] Bezergianni S, Kalogianni A. Hydrocracking of used cooking oil for biofuels production. Bioresour Technol 2009;100:3927–32.
[10] Bezergianni S, Kalogianni A, Vasalos IA. Hydrocracking of vacuum gas oil-vegetable oil mixtures for biofules production. Bioresour Technol 2009;100:3036–42.
[11] Bezergianni S, Voutetakis S, Kalogianni A. Catalytic hydrocracking of fresh and used cooking oil. Ind Eng Chem Res 2009;48:8402–6.
[12] Robota HJ, Alger JC, Shafer L. Converting algal triglycerides to diesel and HEFA jet fuel fractions. Energy Fuels 2013;27:985–96.
[13] Daroch M, Geng S, Wang GY. Recent advances in liquid biofuel production from algal feedstocks. Appl Energy 2013;102:1371–81.
[14] Serrano-Ruiz JC, Ramos-Fernández EV, Sepúlveda-Escribano A. From biodiesel and bioethanol to liquid hydrocarbon fuels: new hydrotreating and advanced microbial technologies. Energy Environ Sci 2012;5:5638–52.
[15] Kumabe K, Sato T, Matsumoto K, Ishida Y, Hasegawa T. Production of hydrocarbons in Fischer-Tropsch synthesis with Fe-based catalyst: investigations of primary kerosene yield and carbon mass balance. Fuel 2010;89:2088–95.
[16] Dupain X, Krul RA, Makkee M, Moulijn JA. Are Fischer-Tropsch waxes good feedstocks for fluid catalytic cracking units? Catal Today 2005;106:288–92.
[17] Naik CV, Puduppakkam KV, Modak A, Meeks E, Wang YL, Feng QY, et al. Detailed chemical kinetic mechanism for surrogates of alternative jet fuels. Combust Flame 2011;158:434–45.
[18] Lobo P, Hagen DE, Whitefield PD. Comparison of PM emissions from a commercial jet engine burning conventional, biomass, and Fischer-Tropsch fuels. Environ Sci Technol 2011;45:10744–9.
[19] Corporan E, Edwards T, Shafer L, DeWitt MJ, Klingshirn C, Zabarnick S, et al. Chemical, thermal stability, seal swell, and emissions studies of alternative jet fuels. Energy Fuels 2011;25:955–66.
[20] Huber GW, Iborra S, Corma A. Synthesis of transportation fuels from biomass: chemistry, catalysts, and engineering. Chem Rev 2006;106:4044–98.
[21] Olcay H, Subrahmanyam AV, Xing R, Lajoie J, Dumesic JA, Huber GW. Production of renewable petroleum refinery diesel and jet fuel feedstocks from hemicellulose sugar streams. Energy Environ Sci 2013;6:205–16.
[22] Corbetta M, Manenti F, Pirola C, Tsodikov MV, Chistyakov AV. Aromatization of propane: techno-economic analysis by multiscale "kinetics-to-process" simulation. Comput Chem Eng 2014;71:457–66.
[23] Price GL, Kanazirev V. Ga_2O_3/HZSM-5 propane aromatization catalysts: formation of active centers via solid-state reaction. J Catal 1990;126:267–78.
[24] Demirbas MF. Biorefineries for biofuel upgrading: a critical review. Appl Energy 2009;86:151–61.
[25] Xu Y, Wang TJ, Ma LL, Zhang Q, Liang W. Upgrading of the liquid fuel from fast pyrolysis of biomass over MoNi/γ-Al_2O_3 catalysts. Appl Energy 2010;87:2886–91.
[26] Mortensen PM, Grunwaldt JD, Jensen PA, Knudsen KG, Jensen AD. A review of catalytic upgrading of bio-oil to engine fuels. Appl Catal A 2011;407:1–19.
[27] Bykova MV, Ermakov DY, Kaichev VV, Bulavchenko OA, Saraev AA, Lebedev MY, et al. Ni-based sol–gel catalysts as promising systems for crude bio-oil upgrading: guaiacol hydrodeoxygenation study. Appl Catal B 2012;113:296–307.
[28] Huang WW, Gong FY, Fan MH, Zhai Q, Hong CG, Li QX. Production of light olefins by catalytic conversion of lignocellulosic biomass with HZSM-5 zeolite impregnated with 6 wt.% lanthanum. Bioresour Technol 2012;121:248–55.
[29] Gong FY, Yang Z, Hong CG, Huang WW, Ning S, Zhang ZX, et al. Selective conversion of bio-oil to light olefins: controlling catalytic cracking for maximum olefins. Bioresour Technol 2011;102:9247–54.
[30] Han DD, Row KH. Recent applications of ionic liquids in separation technology. Molecules 2010;15:2405–26.
[31] Olivier-Bourbigou H, Magna L, Morvan D. Ionic liquids and catalysis: recent progress from knowledge to applications. Appl Catal A 2010;373:1–56.
[32] Corma A, García H. Lewis acids: from conventional homogeneous to green homogeneous and heterogeneous catalysis. Chem Rev 2003;103:4307–65.
[33] Muginova SV, Galimova AZ, Polyakov AE, Shekhovtsova TN. Ionic liquids in enzymatic catalysis and biochemical methods of analysis: capabilities and prospects. J Anal Chem 2010;65:331–51.
[34] Liu DJ, Zhang YT, Chen EYX. Organocatalytic upgrading of the key biorefining building block by a catalytic ionic liquid and N-heterocyclic carbenes. Green Chem 2012;14:2738–46.

[35] Yuan LX, Chen YQ, Song CF, Ye TQ, Guo QX, Zhu QS, et al. Electrochemical catalytic reforming of oxygenated-organic compounds: a highly efficient method for production of hydrogen from bio-oil. Chem Commun 2008;41:5215–7.
[36] Hou T, Yuan LX, Ye TQ, Gong L, Tu J, Yamamoto M, et al. Hydrogen production by low-temperature reforming of organic compounds in bio-oil over a CNT-promoting Ni catalyst. Int J Hydrogen Energy 2009;34:9095–107.
[37] Kan T, Xiong JX, Li XL, Ye TQ, Yuan LX, Torimoto Y, et al. High efficient production of hydrogen from crude bio-oil via an integrative process between gasification and current-enhanced catalytic steam reforming. Int J Hydrogen Energy 2010;35:518–32.
[38] Xu Y, Ye TQ, Qiu SB, Ning S, Gong FY, Liu Y, et al. High efficient conversion of CO_2-rich bio-syngas to CO-rich bio-syngas using biomass char: a useful approach for production of bio-methanol from bio-oil. Bioresour Technol 2011;102:6239–45.
[39] Fan MH, Jiang PW, Bi PY, Deng SM, Yan LF, Zhai Q, et al. Directional synthesis of ethylbenzene through catalytic transformation of lignin. Bioresour Technol 2013;143:59–67.
[40] Dagaut P, Cathonnet M. The ignition, oxidation, and combustion of kerosene: a review of experimental and kinetic modeling. Prog Energy Combust Sci 2006;32:48–92.
[41] Vukadinovic V, Habisreuther P, Zarzalis N. Influence of pressure and temperature on laminar burning velocity and Markstein number of kerosene Jet A-1: experimental and numerical study. Fuel 2013;111:401–10.
[42] de Lucas A, Canizares P, Durán A, Carrero A. Dealumination of HZSM-5 zeolites: effect of steaming on acidity and aromatization activity. Appl Catal A 1997;154:221–40.
[43] Gayubo AG, Aguayo AT, Atutxa A, Prieto R, Bilbao J. Role of reaction-medium water on the acidity deterioration of a HZSM-5 zeolite. Ind Eng Chem Res 2004;43:5042–8.
[44] Yang YL, Kou Y. Determination of the Lewis acidity of ionic liquids by means of an IR spectroscopic probe. Chem Commun 2004;2:226–7.
[45] Blanco CG, Banciella DC, Azpíroz MDG. Alkylation of naphthalene using three different ionic liquids. J Mol Catal A: Chem 2006;253:203–6.
[46] American Society for Testing and Materials (ASTM). Standard specification for aviation turbine fuel containing synthesized hydrocarbons. West Conshohocken, PA: ASTM; 2009.